Structural Origins for Tunable Open-Circuit Voltage in Ternary-Blend Organic Solar Cells

*Petr P. Khlyabich, Andrey E. Rudenko, Barry C. Thompson, and Yueh-Lin Loo**

Ternary-blend bulk-heterojunction solar cells have provided a unique opportunity for tuning the open-circuit voltage (V_{oc}) as the "effective" highest occupied molecular orbital (HOMO) or lowest unoccupied molecular orbital (LUMO) energy levels shift with active-layer composition. Grazing-incidence X-ray diffraction (GIXD) measurements performed on such ternary-blend thin films reveal evidence that the two polymer donors interact intimately; their ionization potentials are thus reflections of the blend compositions. In ternary-blend thin films in which the two polymer donors do not interact physically, the polymer donors each retain their molecular electronic character; solar cells constructed with these ternary blends thus exhibit V_{oc}s that are pinned to the energy level difference between the highest of the two lying HOMO and the LUMO of the electron acceptor. These observations are consistent with the organic alloy model proposed earlier. Quantification of the square of the square-root differences of the surface energies of the components provides a proxy for the Flory–Huggins interaction parameter for polymer donor pairs in these ternary-blend systems. Of the three ternary-blend systems examined herein, this quantity has to be below 0.094 in order for ternary-blend solar cells to exhibit tunable V_{oc}.

1. Introduction

Organic solar cells provide an attractive platform for energy conversion, given the promise of processing ease, mechanical flexibility, and lightweight form factor.[1–3] The predicted practical efficiency limit for single-junction organic solar cells whose absorbing layers comprise bulk-heterojunctions (BHJ) of a donor and acceptor pair is in the 10%–12% range, even though higher efficiencies are potentially achievable.[4–8] The efficiency can be pushed to 14%–15% for solar cells with a tandem architecture in which two absorbing layers are connected in series or parallel.[4,6,9,10] However, tandem organic solar cells lose one of the main attractive features of organic photovoltaics (OPVs), trading fabrication, and processing ease for a boost in efficiency.

Dr. P. P. Khlyabich, Prof. Y.-L. Loo
Department of Chemical and Biological Engineering
Princeton University
Princeton, NJ 08544, USA
E-mail: lloo@princeton.edu
Dr. A. E. Rudenko, Prof. B. C. Thompson
Department of Chemistry and Loker Hydrocarbon Research Institute
University of Southern California
Los Angeles, CA 90089-1661, USA

DOI: 10.1002/adfm.201502287

Organic BHJ solar cells comprising ternary-blend absorbing layers, based either on two donors and one acceptor or one donor and two acceptors, provide an attractive and effective pathway to increase efficiencies while preserving processing simplicity.[11–22] In early studies, the efficiency enhancement of such solar cells was attributed to an increase in the spectral response upon the introduction of an additional donor having an absorption profile that is complementary to that of the parent donor–acceptor pair, effectively increasing the number of harvested photons and ultimately the photocurrent.[11,13,16,18] Until recently, the open-circuit voltage (V_{oc}) of such devices was thought to be pinned by the difference in the energy levels of the lowest unoccupied molecular orbital (LUMO) of the acceptor and the higher of the two highest occupied molecular orbitals (HOMO) in active layers comprising an acceptor and two donors.[23] Given that the third component that is introduced often has a smaller bandgap than the parent donor in order extend the spectral response of the existing active layer, it almost always has a higher lying HOMO compared to the parent donor. As such, the V_{oc} of these devices are generally smaller than the V_{oc} of counterpart solar cells comprising only the parent donor–acceptor pair.[13,14,18,23–26]

With a series of papers, Thompson and co-workers[11,12,19,27–30] demonstrated that the V_{oc} of ternary-blend solar cells need not be pinned by the smallest energy level difference of the constituents, as described above. In fact, with proper selection of materials combination for ternary-blend active layers, the V_{oc} of these solar cells can be continuously tuned with composition between those derived from the HOMO energy levels of the individual donors. As such, the increase in short-circuit current densities (J_{sc}) with the introduction of a third constituent in these solar cells need not come at the expense of V_{oc}'s that are pinned to the smallest energy level difference of the constituents. By breaking this paradigm, Thompson and co-workers showed that ternary-blend solar cells with efficiencies exceeding parent binary-blend solar cells while maintaining high fill factor (FF) can be made across the blend composition while maintaining the simplicity of processing. Since this discovery, numerous other materials combinations have demonstrated tunable V_{oc} in devices having ternary-blend BHJs.[11,17,27,31–34] Equally many other materials combinations have resulted in ternary-blend solar cells whose V_{oc} is pinned to the smallest

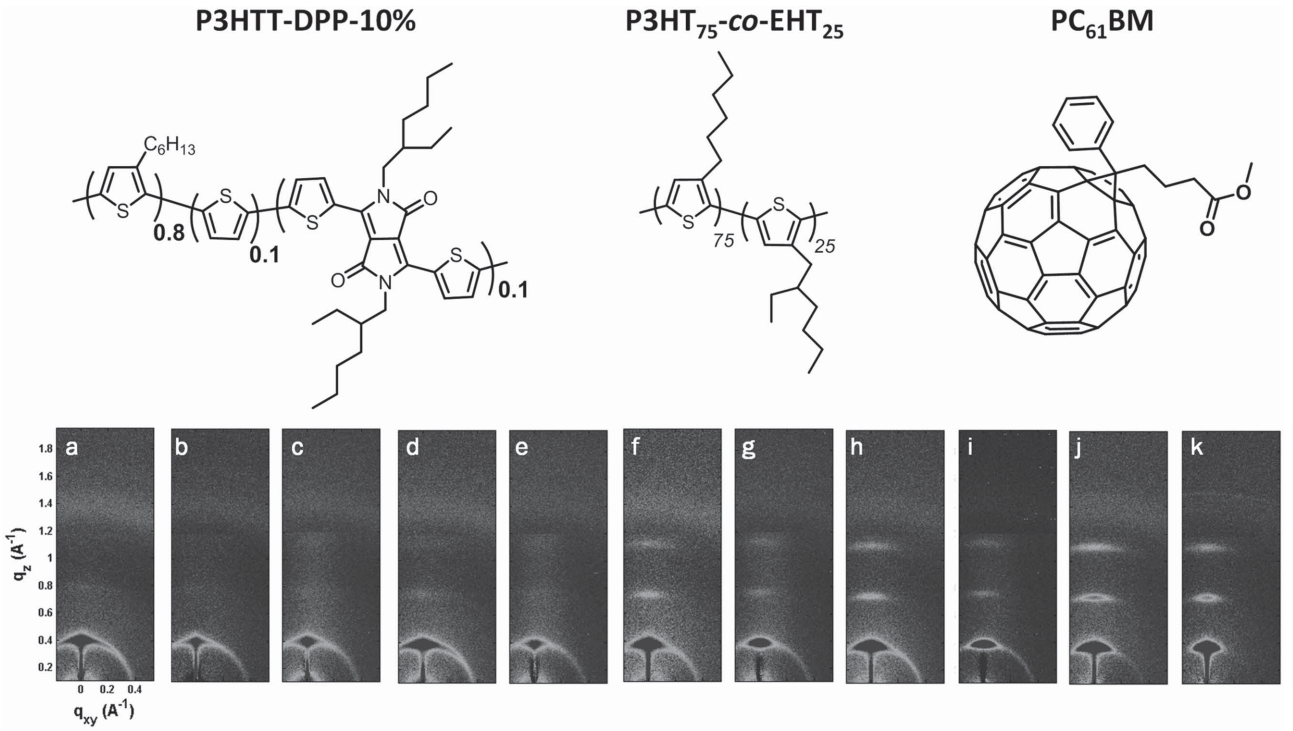

Figure 1. Chemical structures of P3HTT-DPP-10%, P3HT$_{75}$-*co*-EHT$_{25}$ and PC$_{61}$BM and GIXD images of films containing ternary blends of P3HTT-DPP-10%, P3HT$_{75}$-*co*-EHT$_{25}$ and PC$_{61}$BM, at weight ratios of a) 1:0:1.3 (P3HTT-DPP-10%:P3HT$_{75}$-*co*-EHT$_{25}$:PC$_{61}$BM); b) 0.9:0.1:1.1; c) 0.8:0.2:1.0; d) 0.7:0.3:1.0; e) 0.6:0.4:1.0; f) 0.5:0.5:0.9; g) 0.4:0.6:0.9; h) 0.3:0.7:0.8; i) 0.2:0.8:0.8; j) 0.1:0.9:0.9; k) 0:1:0.8.

energy level difference between the HOMO and LUMO of the donor and acceptor constituents, respectively.[13,14,35,36] Understanding the morphological origins of this phenomenon should bring about predictive power for designing materials combination that routinely yield solar cells with high photocurrent without compromising V_{oc}.

Morphological studies on ternary-blend BHJ active layers performed to-date have only examined materials combinations that, when incorporated in devices, resulted in pinned V_{oc}'s. Further, these studies were only conducted on active layers in which the third component comprises <20 wt% of the blends.[24,37–44] While increases in crystallinity and spatial distribution of the third component are said to be responsible for the J_{sc} increase in these ternary-blend solar cells,[24,37] these studies do not comment on how active layer morphology influences V_{oc}.

While morphological studies on materials combinations that result in solar cells exhibiting V_{oc}'s that are tunable with blend composition have not been reported, an organic alloy model[12,19,45] has been proposed on the basis that an average HOMO and an average LUMO energy level must exist in these BHJ active layers and that these energy levels must be composition dependent. That these blends exhibit average HOMOs and average LUMOs that are composition dependent, as opposed to the distinct HOMOs and LUMOs of the constituents, was borne out by photocurrent spectral response (PSR) measurements showing that the energy of the charge-transfer (CT) state in these blends vary continuously with composition.[12,19,30] By implication, constituent miscibilities in such ternary blends must play an important role in determining their electronic structures.[30]

Here, we investigate the morphology of three-component materials combinations, that when incorporated as BHJ active layers in solar cells, result in devices that show variable V_{oc} with blend composition. For reference, we have also characterized the morphology of a ternary blend that resulted in solar cells having composition independent, pinned V_{oc}. Per prior reports, the processing and composition of these blends have been individually optimized so the devices comprising them maintain high J_{sc} and FF. In all the blends investigated for this study, poly(3-hexylthiophene-thiophene-diketopyrrolopyrrole), P3HTT-DPP-10%,[46] is our parent donor polymer and phenyl-C$_{61}$-butyric acid methyl ester (PC$_{61}$BM) is the acceptor. Ternary blend A comprises the addition of poly(3-hexylthiophene-*co*-3-(2-ethylhexyl)thiophene), P3HT$_{75}$-*co*-EHT$_{25}$;[47] devices comprising ternary blend A exhibits composition-dependent V_{oc}. In ternary blend B, the third constituent is poly[*N*-9′-heptadecanyl-2,7-carbazole-*alt*-5,5-(4′,7′-di-2-thienyl-2′,1′,3′-benzothiadiazole)], PCDTBT;[48] devices having ternary blend B as active layers instead show pinned V_{oc}'s. Finally, we also examined the morphology of ternary blend C, whose third component is poly(3-hexylthiophene-thiophene-thienopyrroledione), P3HTT-TPD-10%;[49] these devices exhibit composition-dependent V_{oc}.

2. Results and Discussions

Figure 1 contains the X-ray diffraction images acquired on films comprising ternary blend A with increasing P3HT$_{75}$-*co*-EHT$_{25}$ fraction. These films were processed in a manner identical to those in devices from which the V_{oc}s were extracted.

As reference, we have included the grazing-incidence X-ray diffraction (GIXD) patterns of the polymer donor constituents in Figure S1a,b (Supporting Information). Both polymer donors are crystalline, as evidenced by the presence of strong out-of-plane reflections; the GIXD patterns also reveal higher order reflections, indicating that the polymer donors exhibit long-range order. Quantification of these GIXD patterns reveal the positions of the out-of-plane reflections associated with the polymer donors, with the (100) and (200) reflections of P3HTT-DPP-10% located at 0.41 $Å^{-1}$ and 0.81 $Å^{-1}$ and those of $P3HT_{75}$-*co*-EHT_{25} located at 0.38 $Å^{-1}$ and 0.76 $Å^{-1}$, respectively. The GIXD images, taken on binary blends comprising $PC_{61}BM$ and each of the polymer donors, in Figure 1a,k, look qualitatively similar to those in Figure S1a,b (Supporting Information). This observation indicates that the polymer donor constituents each retain their crystallinities upon introduction of $PC_{61}BM$. The GIXD images of ternary blend A with increasing $P3HT_{75}$-*co*-EHT_{25} fraction are provided in Figure 1b through 1j. We observe one set of reflections, whose positions are between those of the polymer donor constituents that shift monotonically with composition. This trend is more clearly seen in the out-of-plane line cuts in Figure S2 (Supporting Information), which were extracted from the corresponding X-ray diffraction patterns in the vicinity of the reflections, and is quantified by tracking the scattering vector, q_z, in **Figure 2**a and Figure S3 (Supporting Information). Our data thus suggest that the two polymer donors interact, resulting in changes in the characteristic spacing of the crystallites upon the addition of $P3HT_{75}$-*co*-EHT_{25}.

We have also quantified the full width at half the maximum (FWHM) intensity of the X-ray diffraction peaks shown in Figure S2 (Supporting Information); the FWHM of the peaks associated with the (100) and (200) reflections are tracked as a function of $P3HT_{75}$-*co*-EHT_{25} content in Figure 2a and Figure S3, Supporting Information, respectively. First, we notice that the FWHM is uniformly narrow; the quantities are in fact comparable to those associated with the (100) and (200) reflections of P3HT in binary blends of P3HT:$PC_{61}BM$ (0.040 $Å^{-1}$ and 0.047 $Å^{-1}$, respectively). Moreover, the FWHM extracted from the ternary-blend data are flanked by those of the binary blends comprising the polymer donor constituents and $PC_{61}BM$, suggesting that the introduction of the third component does not substantially perturb the crystallite correlation lengths (CCL) in the out-of-plane direction. We have estimated the CCL from the FWHM per Scherrer equation;[50] our data indicate that the CCL in the ternary blends is smaller than those exhibited by the crystallites of $P3HT_{75}$-*co*-EHT_{25} but larger than those exhibited by the crystallites of P3HTT-DPP-10%.

Figure 2b tracks the V_{oc} of solar cells comprising ternary blend A as a function of $P3HT_{75}$-*co*-EHT_{25}.[11] The V_{oc} is continuously tunable spanning a 15% change over the entire composition window. This increase in V_{oc} is consistent with a decrease in the average ionization potential (IP) of the polymer donors, shown also in Figure 2b. A progressively decreasing IP with increasing $P3HT_{75}$-*co*-EHT_{25} content translates to a larger energy difference between the LUMO of $PC_{61}BM$ and the ensemble-average and composition-specific HOMO of the polymer donors, leading to a correspondingly increasing V_{oc} in devices. Consistent with our structural characterization, that

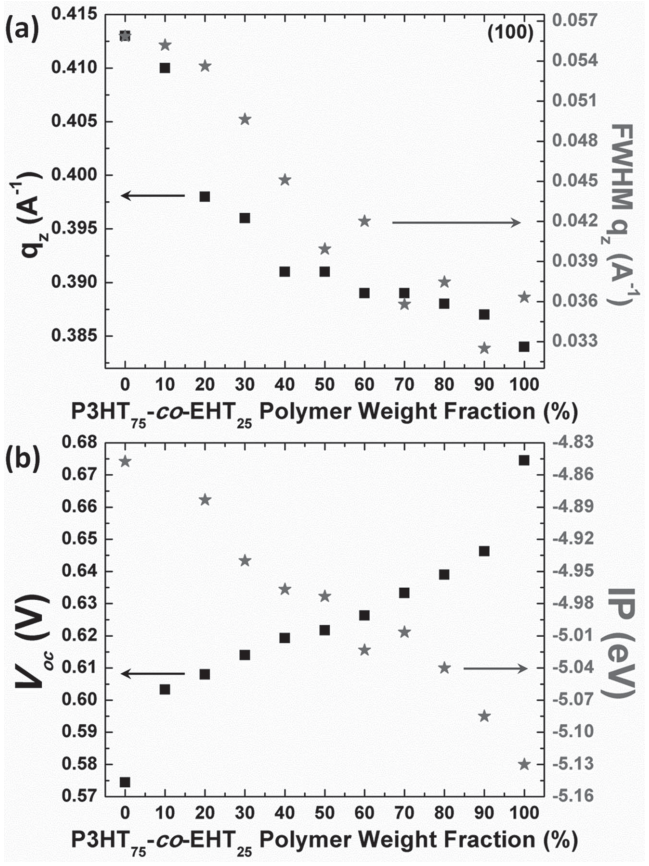

Figure 2. a) Position of the primary reflection (squares) and FWHM (stars) of the primary reflection extracted from the GIXD of the ternary-blend films, containing P3HTT-DPP-10%, $P3HT_{75}$-*co*-EHT_{25} and $PC_{61}BM$, as a function of the fraction of $P3HT_{75}$-*co*-EHT_{25}. b) Open-circuit voltage (V_{oc}) (squares) of ternary-blend BHJ solar cells and ionization potential (stars) of blends of the two polymer donors as a function of the fraction of $P3HT_{75}$-*co*-EHT_{25}.

the IP of the polymer blends is continuously tunable across the composition window suggests mixing of the polymer donors in ternary blend A. While the IP changes by 280 meV over the entire composition range, the V_{oc} of corresponding devices only increases by 100 meV over the same composition range. That the absolute magnitude of change differs likely stems from structural and electronic changes at the donor–acceptor interface with composition. In contrast, the energy of the CT state, which solely reflects the energetics at the donor–acceptor interface, changes by the same amount as the V_{oc}.[12]

Figure 3 contains the chemical structures of the constituents of ternary blend B, its structural characterization, and the evolution of V_{oc} with active-layer composition of solar cells comprising this ternary blend. Different from devices comprising ternary blend A, solar cells comprising ternary blend B exhibit composition-invariant V_{oc} that is not different from the V_{oc} of P3HTT-DPP-10%:$PC_{61}BM$ solar cells (V_{oc} = 0.57 V).[30] Given that the HOMO energy level of P3HTT-DPP-10% is higher than that of PCDTBT, it thus appears that the V_{oc} of solar cells comprising ternary blend B is pinned to the higher lying HOMO of P3HTT-DPP-10%. This characteristically different behavior in V_{oc} compared to solar cells comprising ternary blend A is

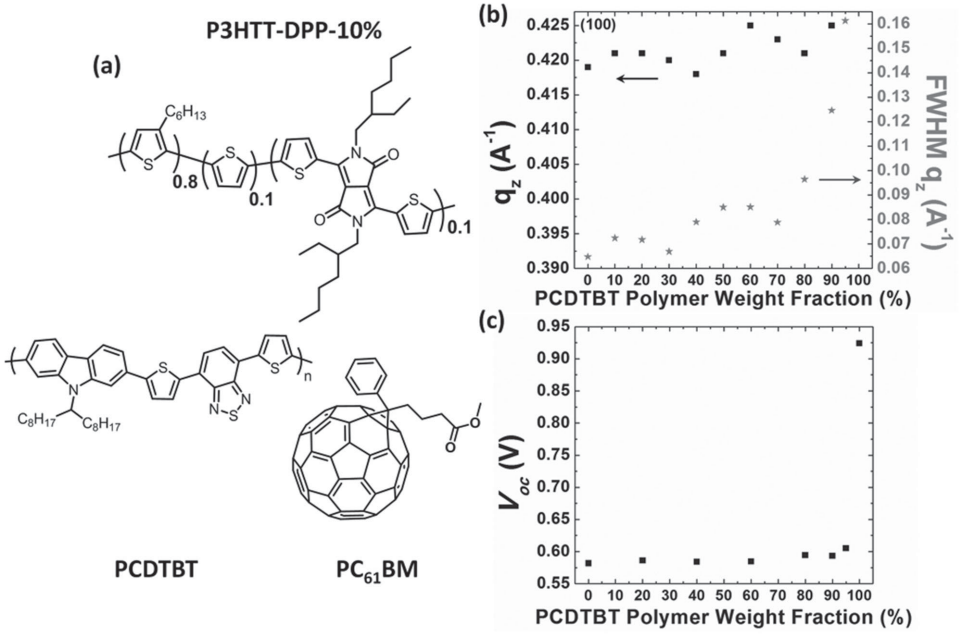

Figure 3. a) Chemical structures of P3HTT-DPP-10%, PCDTBT and $PC_{61}BM$. b) The position of the primary reflection (squares) and FWHM (stars) of the primary reflection of P3HTT-DPP-10% extracted from the GIXD images of the ternary-blend films as a function of the fraction of PCDTBT (only P3HTT-DPP-10% is crystalline; PCDTBT is amorphous). c) Open-circuit voltage (V_{oc}) of ternary-blend BHJ solar cells as a function of the fraction of PCDTBT.

accompanied by differences in the morphology of these active layers. These data are consistent with earlier PSR measurements on the same blend that suggests an absence of mixing between the two polymer donors.[12] The presence of two CT states originating from the two polymer donors, rather than one composition-dependent CT state, as in case of ternary blend A, mandates that hole transport is dominated by the higher HOMO energy level of the two polymer donors (that of P3HTT-DPP-10%). The GIXD patterns corresponding to ternary blend B as a function of composition are shown in Figure S4 (Supporting Information); the GIXD pattern of PCDTBT is shown in Figure S1c (Supporting Information) for completeness. We see that PCDTBT is amorphous under the conditions in which the active layers for solar cells are processed. The out-of-plane reflection observed in the GIXD patterns in Figure S4 (Supporting Information) must thus stem from crystalline P3HTT-DPP-10%. The out-of-plane line cuts extracted from these X-ray diffraction patterns are provided in Figure S5 (Supporting Information). As the concentration of PCDTBT is increased, we observe a gradual decrease in the intensity of the peak corresponding to the (100) reflection of P3HTT-DPP-10%, indicating that the films become progressively less crystalline. This decrease in crystallinity, however, is less than one would expect based on composition alone. Interestingly, the position of this (100) reflection is retained on dilution with PCDTBT.[51] This trend is quantified in Figure 3b in which the out-of-plane scattering vector, q_z, is tracked with composition. This observation is strikingly different from the structural evolution of ternary blend A and suggests that while there may be less P3HTT-DPP-10% crystallites with increasing PCDTBT in films comprising ternary blend B, the crystallites that exist preserve the out-of-plane periodicity. Figure 3b also tracks the FWHM of the peak associated with the (100) reflection of P3HTT-DPP-10% in ternary blend B with composition. The FWHM resembles that of P3HTT-DPP-10% and remains largely independent of concentration up to 70 wt% loading of PCDTBT, above which it increases dramatically. This observation indicates that the CCL of P3HTT-DPP-10% remains largely constant up to this threshold loading of PCDTBT. The decrease in peak intensity of the (100) must thus reflect a progressive decrease the number of crystallites present, as opposed to thinning of crystallites. Different from our findings with ternary blend A, this study suggests little interaction between the two polymer donors in ternary blend B; the addition of PCDTBT to the parent donor–acceptor pair does little to change the crystallite structure of P3HTT-DPP-10%. Accordingly, the V_{oc} of solar cells comprising ternary blend B are dictated by the energy level difference between the LUMO of $PC_{61}BM$ and the higher lying HOMO of the two polymer donor constituents, in this case P3HTT-DPP-10%.

We also characterized the structural evolution of ternary blend C with composition. **Figure 4**a contains the chemical structures of the constituents of ternary blend C. Like in ternary blend A, both polymer donor constituents here are crystalline, exhibiting distinct out-of-plane reflections in their X-ray diffraction patterns (see Figure S1a,d, Supporting Information). The GIXD patterns taken on ternary blend C as a function of composition are provided in Figure S6 (Supporting Information); the corresponding out-of-plane line cuts are provided in Figure S7 (Supporting Information). We observe from Figure S7 (Supporting Information) that the two peaks associated with the (100) reflections of P3HTT-DPP-10% at 0.41 $Å^{-1}$ and

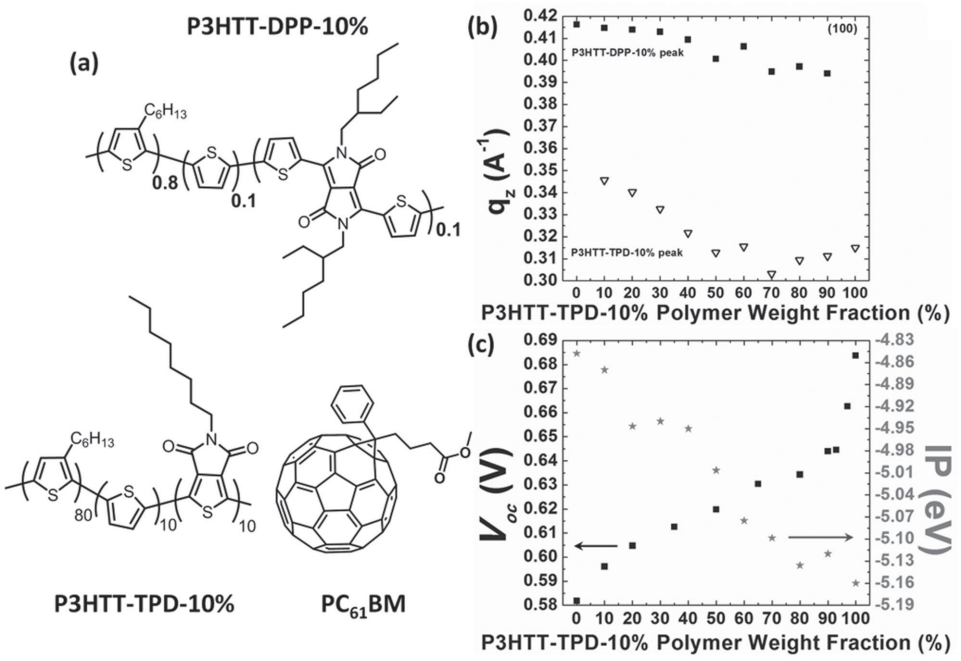

Figure 4. a) Chemical structures of P3HTT-DPP-10%, P3HTT-TPD-10% and $PC_{61}BM$. b) The positions of the primary reflections of P3HTT-DPP-10% (solid squares) and P3HTT-TPD-10% (open triangles) from GIXD images of the ternary-blends films as a function of the fraction of P3HTT-TPD-10%. c) Open-circuit voltage (V_{oc}) (squares) of ternary-blend BHJ solar cells and ionization potential (stars) of blends of the two polymer donor as a function of the fraction of P3HTT-TPD-10%.

P3HTT-TPD-10% at 0.31 $Å^{-1}$ are largely retained, though they shift progressively towards each other on dilution. This trend is quantified by tracking q_z as a function of composition in Figure 4b. This shift in q_z suggests that P3HTT-DPP-10% crystallites are able to accommodate P3HTT-TPD-10% on dilution and vice versa. Given that the primary peak of P3HTT-TPD-10% shifts by over 12% over the composition window whereas the primary peak of P3HTT-DPP-10% only shifts by 5% over that same composition range, P3HTT-TPD-10% is more able to accommodate P3HTT-DPP-10% than P3HTT-DPP-10% is at accommodating P3HTT-TPD-10% in their respective crystal structures on dilution. Figure 4c tracks the V_{oc} of solar cells comprising ternary blend C as a function of composition.[28] We observe that the V_{oc} is tunable across the composition window, not unlike what we had observed for devices with ternary blend A. This V_{oc} tunability originates from an "effective" IP that can be continuously increased as P3HTT-TPD-10% is added to the parent donor-acceptor pair of P3HTT-DPP-10%:$PC_{61}BM$.

Collectively, the structural evolution of ternary blends A, B, and C with composition implicates the key role of polymer–polymer interactions in determining the V_{oc} behavior in ternary-blend solar cells. When the polymer donor constituents interact, as noted by the accommodation of one polymer into another's existing crystal structure in ternary blends A and C, we measure an ensemble-average IP that is tunable within the range bracketed by the IPs of the polymer donor constituents. Accordingly, solar cells comprising these ternary blends exhibit tunable V_{oc} that can be tracked to changes in the effective IP. The polymer donor constituents in ternary blend B, however, do not interact. Solar cells comprising ternary blend B are thus pinned to the energy difference between the LUMO of the acceptor and the higher lying HOMO of the two donor constituents.

It is therefore not surprising that surface energy differences between the constituents of these ternary blends provide a good indication of whether the blends would result in solar cells having pinned or tunable V_{oc}. The surface energies of P3HTT-DPP-10% is reported to be 19.9 mN m^{-1} and those of $P3HT_{75}$-*co*-EHT_{25} and P3HTT-TPD-10% are 22.1 mN m^{-1} and 20.7 mN m^{-1}, respectively, whereas that of PCDTBT is 29.5 mN m^{-1}.[28,30] The surface energy difference between the polymer donor constituents in ternary blends A and C (2.2 and 0.8 mN m^{-1}, respectively) are thus small compared to that between the polymer donor constituents in ternary blend B (9.6 mN m^{-1}). We can alternatively invoke the Flory–Huggins interaction parameter to quantify the interactions between these polymer donor constituents. The Flory–Huggins interaction parameter is proportional to the square of the square-root differences of the surface energies of the components in question.[52] As a proxy for the Flory-Huggins interaction parameter, the absolute measurement of which is difficult given the polymers in hand, we have quantified the square of the square-root differences of the surface energies in **Table 1** for the three blends under study here. We see that this quantity is 0.058 for the polymer constituents in ternary blend A, 0.094 and 0.008 for those in ternary blends B and C, respectively. The idea that polymer donor interactions are key in dictating the V_{oc} behavior in the resulting ternary-blend solar cells is further consistent with the organic alloy model and the PSR measurements[12,19] that a single charge transfer state is detected in ternary blends A and C whose energy is continuously tunable with composition.

Table 1. Open-circuit voltage (V_{oc}) tunability and the square of the square-root differences of surface energy of the polymer donor pairs in the ternary blends examined in this study.

Polymer:polymer pairs	V_{oc} Tunability	$\chi_{AB} \approx (\sqrt{\gamma_A} - \sqrt{\gamma_B})^2$
P3HTT-DPP-10%:P3HT$_{75}$-*co*-EHT$_{25}$	Tunable	0.058
P3HTT-DPP-10%:P3HTT-TPD-10%	Tunable	0.008
P3HTT-DPP-10%:PCDTBT	Pinned	0.094

Surface energies (γ_A, γ_B) for neat constituents are from refs.[28,29]

3. Conclusion

In summary, we have performed the first direct structural study of ternary-blend BHJ active layers whose solar cells demonstrate tunable V_{oc}. Our structural studies suggest that some level of molecular mixing between the polymer donor constituents are necessary in order to tune the V_{oc} of solar cells comprising these materials combinations. While quantifying the Flory–Huggins interaction parameter is difficult with these polymer donor pairs, the extent of molecular mixing can be quantified by the square of square-root differences in the surface energies as a proxy. Comparison across the three ternary blends under study suggests this quantity needs to be below 0.094 for materials combination to exhibit tunable V_{oc} when incorporated into solar cells.

4. Experimental Section

Materials: All reagents from commercial sources were used without further purification, unless otherwise noted. Solvents were purchased from VWR and used without further purification except for THF, which was dried over sodium/benzophenone before distillation.

Synthetic Procedures: The synthesis of P3HTT-DPP-10%, P3HTT-TPD-10%, P3HT$_{75}$-*co*-EHT$_{25}$, and PCDTBT, followed reported procedures in the literature without further modification.[30,46,47,49]

Thin Films: Indium tin oxide (ITO)-coated glass substrates (Colorado Concept Coatings LLC) were sequentially cleaned by sonication in de-ionized water, acetone, and isopropyl alcohol, and dried in a nitrogen stream. Poly(3,4-ethylenedioxythiophene) polystyrene sulfonate (PEDOT:PSS) (Baytron P VP AI 4083, dispersion filtered with a 0.45 μm polyvinylidene fluoride (PVDF) syringe filter from Pall Life Sciences prior to deposition) was first spin-coated on pre-cleaned ITO-coated glass substrates and baked at 130 °C for 40 min. Individual solutions of P3HTT-DPP-10%, P3HT$_{75}$-*co*-EHT$_{25}$, PCDTBT, P3HTT-TPD-10%, and PC$_{61}$BM were prepared in *o*-dichlorobenzene. The solutions were stirred for 24 h before they were mixed at the desired mass ratios and stirred for 24 h to ensure uniformity. The concentrations and mass ratios were determined to yield optimized solar cells per reports elsewhere.[11,30] Solutions comprising materials combination that yielded the ternary blend thin films were spin-coated after they have been passed through a 0.45 μm polytetrafluorethylene (PTFE) syringe filter from Pall Life Sciences atop PEDOT:PSS. While solution deposition was carried out at ambient conditions, the films were placed in a N_2 cabinet during which residual *o*-dichlorobenzene was allowed to slowly evaporate. Consistent with active layers employed in ternary-blend solar cells, these films were not subjected to further thermal annealing.

GIXD Measurements: GIXD experiments were conducted at the G2 station of the Cornell High Energy Synchrotron Source (CHESS) with X-rays at 10.05 ± 0.01 keV. At the G2 station, the beam was selected to be 0.2 mm tall and 2 mm wide. The beam energy was selected using a beryllium single-crystal monochromator. Scattered intensity was collected using a 640-element 1D diode array. The X-ray beam was aligned above the film's critical angle and below that of the substrate, at 0.16–0.17° with respect to the substrate. Variations in detector-to-sample distance were accounted for during data processing. Additionally, all GIXD images have been background subtracted, and polarization and absorption corrections polarization and absorption corrections were applied during data processing.

Ionization Potential (IP) Measurements: Ambient IP measurements of binary blends of the polymer donors were performed on an AC-2 photoelectron spectrometer from Riken Keiki. These films were prepared as outlined above from *o*-dichlorobenzene solutions at a total polymer concentration of 10 mg mL^{-1}.

Supporting Information

Supporting Information is available from the Wiley Online Library or from the author.

Acknowledgements

GIXD experiments were conducted at the Cornell High Energy Synchrotron Source. The authors acknowledge funding from the National Science Foundation (DMR-1035217 and DMR-0819860) and the Office of Naval Research (N00014-11-10328) for support of P.P.K. and Y.L.L. B.C.T. acknowledges support by the National Science Foundation (CBET Energy for Sustainability) CBET-1436875.

Received: June 4, 2015
Revised: July 10, 2015
Published online: August 6, 2015

[1] L. Dou, J. You, Z. Hong, Z. Xu, G. Li, R. A. Street, Y. Yang, *Adv. Mater.* **2013**, *25*, 6642.
[2] N. E. Jackson, B. M. Savoie, T. J. Marks, L. X. Chen, M. A. Ratner, *J. Phys. Chem. Lett.* **2015**, *6*, 77.
[3] K. A. Mazzio, C. K. Luscombe, *Chem. Soc. Rev.* **2015**, *44*, 78.
[4] R. A. J. Janssen, J. Nelson, *Adv. Mater.* **2013**, *25*, 1847.
[5] M. C. Scharber, N. S. Sariciftci, *Prog. Polym. Sci.* **2013**, *38*, 1929.
[6] J. D. Kotlarski, P. W. M. Blom, *Appl. Phys. Lett.* **2011**, *98*, 053301.
[7] C. Deibel, V. Dyakonov, *Rep. Prog. Phys.* **2010**, *73*, 096401.
[8] N. C. Giebink, G. P. Wiederrecht, M. R. Wasielewski, S. R. Forrest, *Phys. Rev. B* **2011**, *83*, 195326.
[9] M. K. Siddiki, J. Li, D. Galipeau, Q. Qiao, *Energy Environ. Sci.* **2010**, *3*, 867.
[10] T. Ameri, G. Dennler, C. Lungenschmied, C. J. Brabec, *Energy Environ. Sci.* **2009**, *2*, 347.
[11] P. P. Khlyabich, B. Burkhart, B. C. Thompson, *J. Am. Chem. Soc.* **2012**, *134*, 9074.
[12] R. A. Street, D. Davies, P. P. Khlyabich, B. Burkhart, B. C. Thompson, *J. Am. Chem. Soc.* **2013**, *135*, 986.
[13] T. Ameri, J. Min, N. Li, F. Machui, D. Baran, M. Forster, K. J. Schottler, D. Dolfen, U. Scherf, C. J. Brabec, *Adv. Energy Mater.* **2012**, *2*, 1198.
[14] T. Ameri, T. Heumüller, J. Min, N. Li, G. Matt, U. Scherf, C. J. Brabec, *Energy Environ. Sci.* **2013**, *6*, 1796.
[15] T. Ameri, P. Khoram, J. Min, C. J. Brabec, *Adv. Mater.* **2013**, *25*, 4245.
[16] L. Yang, H. Zhou, S. C. Price, W. You, *J. Am. Chem. Soc.* **2012**, *134*, 5432.
[17] J.-H. Huang, M. Velusamy, K.-C. Ho, J.-T. Lin, C.-W. Chu, *J. Mater. Chem.* **2010**, *20*, 2820.

[18] Y. J. Cho, J. Y. Lee, B. D. Chin, S. R. Forrest, *Org. Electron.* **2013**, *14*, 1081.
[19] P. P. Khlyabich, B. Burkhart, A. E. Rudenko, B. C. Thompson, *Polymer* **2013**, *54*, 5267.
[20] S. Liu, P. You, J. Li, J. Li, C.-S. Lee, B. S. Ong, C. Surya, F. Yan, *Energy Environ. Sci.* **2015**, *8*, 1463.
[21] Y. (Michael) Yang, W. Chen, L. Dou, W.-H. Chang, H.-S. Duan, B. Bob, G. Li, Y. Yang, *Nat. Photonics* **2015**, *9*, 190.
[22] L. Lu, T. Xu, W. Chen, E. S. Landry, L. Yu, *Nat. Photonics* **2014**, *8*, 716.
[23] M. Koppe, H.-J. Egelhaaf, G. Dennler, M. C. Scharber, C. J. Brabec, P. Schilinsky, C. N. Hoth, *Adv. Funct. Mater.* **2010**, *20*, 338.
[24] T. Ameri, P. Khoram, T. Heumüller, D. Baran, F. Machui, A. Troeger, V. Sgobba, D. Guldi, M. Halik, S. Rathgeber, U. Scherf, C. J. Brabec, *J. Mater. Chem. A* **2014**, *2*, 19461.
[25] C. Kästner, S. Rathgeber, D. A. M. Egbe, H. Hoppe, *J. Mater. Chem. A* **2013**, *1*, 3961.
[26] G. D. Sharma, S. P. Singh, M. S. Roy, J. A. Mikroyannidis, *Org. Electron.* **2012**, *13*, 1756.
[27] P. P. Khlyabich, B. Burkhart, B. C. Thompson, *J. Am. Chem. Soc.* **2011**, *133*, 14534.
[28] P. P. Khlyabich, A. E. Rudenko, B. Burkhart, B. C. Thompson, *ACS Appl. Mater. Interfaces* **2015**, *7*, 2322.
[29] R. A. Street, P. P. Khlyabich, A. E. Rudenko, B. C. Thompson, *J. Phys. Chem. C* **2014**, *118*, 26569.
[30] P. P. Khlyabich, A. E. Rudenko, R. A. Street, B. C. Thompson, *ACS Appl. Mater. Interfaces* **2014**, *6*, 9913.
[31] H. Li, Z.-G. Zhang, Y. Li, J. Wang, *Appl. Phys. Lett.* **2012**, *101*, 163302.
[32] H. Xu, H. Ohkita, H. Benten, S. Ito, *Jpn. J. Appl. Phys.* **2014**, *53*, 01AB10.
[33] H. Kang, K.-H. Kim, T. E. Kang, C.-H. Cho, S. Park, S. C. Yoon, B. J. Kim, *ACS Appl. Mater. Interfaces* **2013**, *5*, 4401.
[34] L. Chen, K. Yao, Y. Chen, *J. Mater. Chem.* **2012**, *22*, 18768.
[35] J. Lee, M. H. Yun, J. Kim, J. Y. Kim, C. Yang, *Macromol. Rapid Commun.* **2012**, *33*, 140.
[36] H. Cha, D. S. Chung, S. Y. Bae, M.-J. Lee, T. K. An, J. Hwang, K. H. Kim, Y.-H. Kim, D. H. Choi, C. E. Park, *Adv. Funct. Mater.* **2013**, *23*, 1556.
[37] Y. Gu, C. Wang, F. Liu, J. Chen, O. E. Dyck, G. Duscher, T. P. Russell, *Energy Environ. Sci.* **2014**, *7*, 3782.
[38] F. Liu, Y. Gu, X. Shen, S. Ferdous, H.-W. Wang, T. P. Russell, *Prog. Polym. Sci.* **2013**, *38*, 1990.
[39] N. Li, F. Machui, D. Waller, M. Koppe, C. J. Brabec, *Sol. Energy Mater. Sol. Cells* **2011**, *95*, 3465.
[40] J.-S. Huang, T. Goh, X. Li, M. Y. Sfeir, E. A. Bielinski, S. Tomasulo, M. L. Lee, N. Hazari, A. D. Taylor, *Nat. Photonics* **2013**, *7*, 479.
[41] K. R. Graham, R. Stalder, P. M. Wieruszewski, D. G. Patel, D. H. Salazar, J. R. Reynolds, *ACS Appl. Mater. Interfaces* **2013**, *5*, 63.
[42] F. Machui, S. Rathgeber, N. Li, T. Ameri, C. J. Brabec, *J. Mater. Chem.* **2012**, *22*, 15570.
[43] F. Machui, S. Abbott, D. Waller, M. Koppe, C. J. Brabec, *Macromol. Chem. Phys.* **2011**, *212*, 2159.
[44] H. Yan, D. Li, Y. Zhang, Y. Yang, Z. Wei, *J. Phys. Chem. C* **2014**, *118*, 10552.
[45] D. Angmo, M. Bjerring, N. C. Nielsen, B. C. Thompson, F. C. Krebs, *J. Mater. Chem. C* **2015**, *3*, 5541.
[46] P. P. Khlyabich, B. Burkhart, C. F. Ng, B. C. Thompson, *Macromolecules* **2011**, *44*, 5079.
[47] B. Burkhart, P. P. Khlyabich, B. C. Thompson, *Macromolecules* **2012**, *45*, 3740.
[48] S. Beaupré, M. Leclerc, *J. Mater. Chem. A* **2013**, *1*, 11097.
[49] B. Burkhart, P. P. Khlyabich, B. C. Thompson, *ACS Macro Lett.* **2012**, *1*, 660.
[50] A. Sharenko, N. D. Treat, J. A. Love, M. F. Toney, N. Stingelin, T.-Q. Nguyen, *J. Mater. Chem. A* **2014**, *2*, 15717.
[51] Y.-L. Loo, P. P. Khlyabich, *SPIE Newsroom* **2015**, DOI: 10.1117/2.1201502.005789 .
[52] *Polymer Handbook* (Eds: J. Brandrup, E. H. Immergut, E. A. Grulke), 4th ed., Wiley, New York, NY, USA **1999**.